DIAMOND

Intense Blue, with Very High Boron Concentration

Natural blue diamonds are extremely rare in nature and highly desired within the gem industry. One of the world's most famous gemstones, the Hope diamond, is classified as a natural type IIb blue diamond. It contains the impurity boron within the diamond carbon lattice. The presence of boron as an impurity in natural diamond is rare, as the amount of uncompensated boron found is typically less than 0.5 ppm.

Housed in the Smithsonian Institute in Washington, DC, the Hope is part of a collection incorporating many boron-containing natural type IIb diamonds, and has been part of a study relating boron concentrations and the intensity of blue coloration in natural and synthetic diamond (E. Gaillou et al., "Boron in natural type IIb blue diamonds: Chemical and spectroscopic measurements," *American Mineralogist*, Vol. 97, 2012, pp. 1–18).

The East Coast laboratory recently received a 1.18 ct Fancy Intense blue diamond (figure 1) for a colored diamond grading report. The diamond's old European-style cut indicated that this was not a recently faceted gemstone. The clarity was very high, adding to the rarity of this blue diamond. When exposed to short-wave UV fluorescence (about 230 nm), the diamond displayed blue phosphorescence (figure 2). Phosphorescence is a diagnostic feature of natural type IIb diamonds; red phosphorescence is also frequently observed, the most notable example being the Hope diamond.

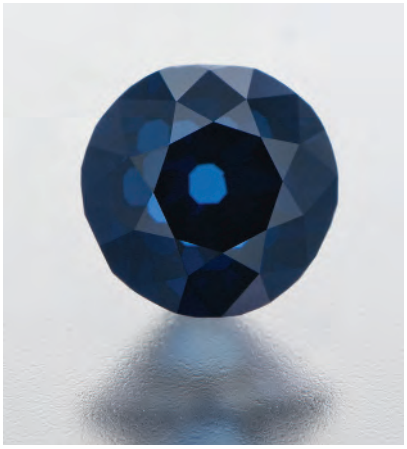

Figure 1. This 1.18 ct Fancy Intense blue diamond was recently seen in the New York lab.

Infrared absorption spectroscopy identified the diamond as type IIb, with a very high concentration of uncompensated boron for a natural diamond, even for a stone with synthetic boron doping (figure 3). Further analysis, including photoluminescence spectroscopy, proved it to be a natural diamond. From the mid-infrared absorption spectrum, we determined a boron concentration of 5.84 ppm atomic. By normalizing the mid-IR spectrum, we obtained the integrated intensity of an absorption peak centered at 1290 cm^{-1} (A.T. Collins, "Determination of the boron concentration in diamond using optical spectroscopy," *Proceedings of the 61st Diamond Conference*, 2010, Warwick, UK). Most documented type IIb diamonds in this color range only have recorded uncompensated boron concentrations between approximately 0.24 and 0.36 ppm (E. Gaillou et al., "Study of the Blue Moon diamond," Spring 2015 *G&G*, pp. 280–286).

This is the highest boron concentration ever reported in a natural diamond. Compared to other docu-

Figure 2. Blue phosphorescence was observed in the DiamondView after the stone's exposure to strong short-wave UV radiation.

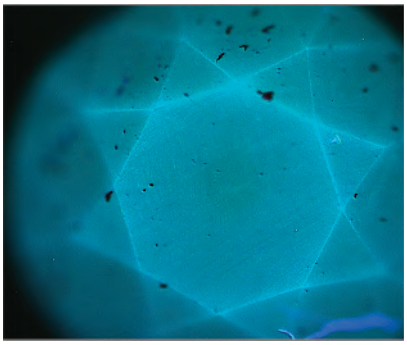

Editors' note: All items were written by staff members of GIA laboratories.

Gems & Gemology, Vol. 51, No. 2, pp. 176–188.

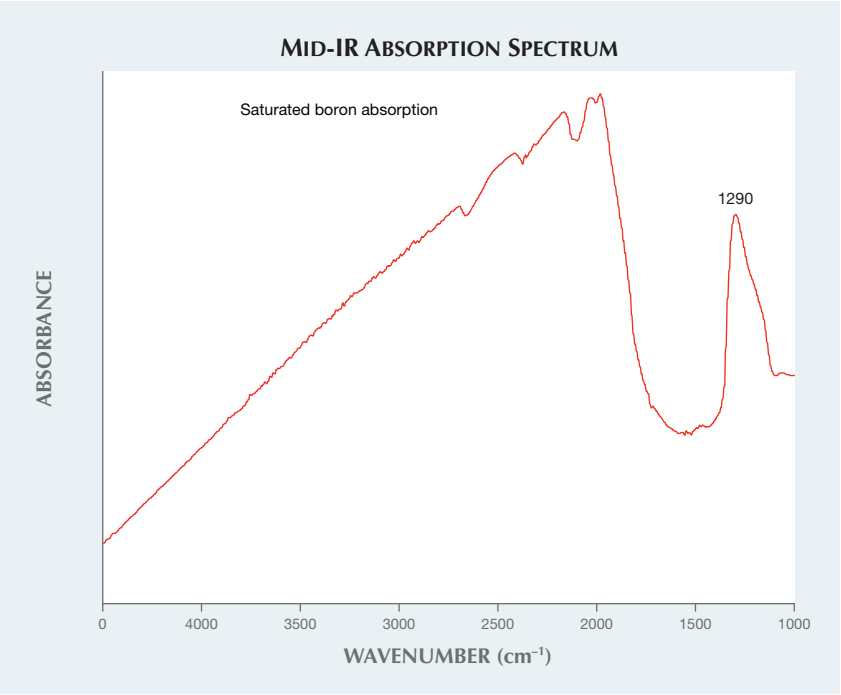

Figure 3. Normalized mid-IR absorption spectrum of the 1.18 ct Fancy Intense blue type IIb diamond, with saturated boron–related absorption and a 1290 cm^{-1} peak.

mented type IIb diamonds, the concentration is staggeringly high. This diamond's intense blue color rivals that of the Hope, leading one to believe that boron contributes strongly to the color of natural blue type IIb diamonds. This has never been proven, however, and there is not a well-defined relationship between blue color and uncompensated boron concentration in diamond (Gaillou et al., 2012).

Further observation and analytical study may prove a correlation between optically active boron and the intensity of blue color in natural diamonds.

Paul Johnson and Wuyi Wang

Rare Type IIb Gray-Purple

Photoluminescence (PL) spectroscopy using several laser excitations has become the most important method for determining diamond color origin. Part of PL analysis is observing peaks that correlate with a diamond's color, type, or other gemological properties, but for which the physical model is still unknown. One such center is the PL peak at 776.4 nm, which is commonly observed in type IIb diamonds with intensely colored (i.e., Fancy to Fancy Deep) blue to gray color and in combination with red phosphorescence (S. Eaton-Magaña and R. Lu, "Phosphorescence in type IIb diamonds," *Diamond and Related Materials*, Vol. 20, No. 7, 2011, pp. 983–989). Recently, the Carlsbad laboratory tested a 1.42 ct colored diamond that showed an extremely strong 776.4 nm emission. Infrared absorption spectroscopy confirmed the specimen as a type IIb natural diamond with a boron concentration of approximately 28 ppb. This stone was notable not only for this intense emission, but also for its Fancy gray-purple color (figure 4). This is an extremely rare combination in a type IIb diamond.

Type IIb diamonds sometimes have a violet color description, but they rarely exhibit hues that are outside the blue-gray-violet range. While the perceived difference between a violet and purple diamond may be quite subtle, it is an important distinction when determining color origin. An additional reddish component that distinguishes purple from violet diamonds is extremely rare among type IIb fancy color diamonds. Other type IIb hues include gray-green or yellowish green (e.g., Summer 2009 Lab Notes, p. 136; Spring 2012 Lab Notes, pp. 47–48). Purple diamonds are quite rare and almost exclusively type Ia, their color deriving from the 550 nm band observed in their visible absorption spectra (S. V. Titkov et al., "Natural-color purple diamonds from Siberia," Spring 2008 *G&G*, pp. 56–64). This absorption band is also the cause of color for many pink to red diamonds; however, the absorption spectrum for this diamond was featureless within the visible range, which is typical for type IIb diamonds. This stone is likely the first purple type IIb diamond examined at GIA.

Figure 4. This 1.42 ct type IIb natural diamond was significant for its unusual Fancy gray-purple color and its strong emission at 776.4 nm under PL spectroscopy.

The diamond had the strongest 776.4 nm PL emission yet observed by the author (figure 5). The configuration of the optical center is unknown but might include a boron-vacancy complex (T. Ardon and S. Eaton-Magaña, "Spatial distribution of boron and PL optical centers in type IIb diamond," 2013 GSA Annual Meeting). Red phosphorescence, centered at 660 nm, was observed using DiamondView and excited by both ultraviolet and visible-light wavelengths

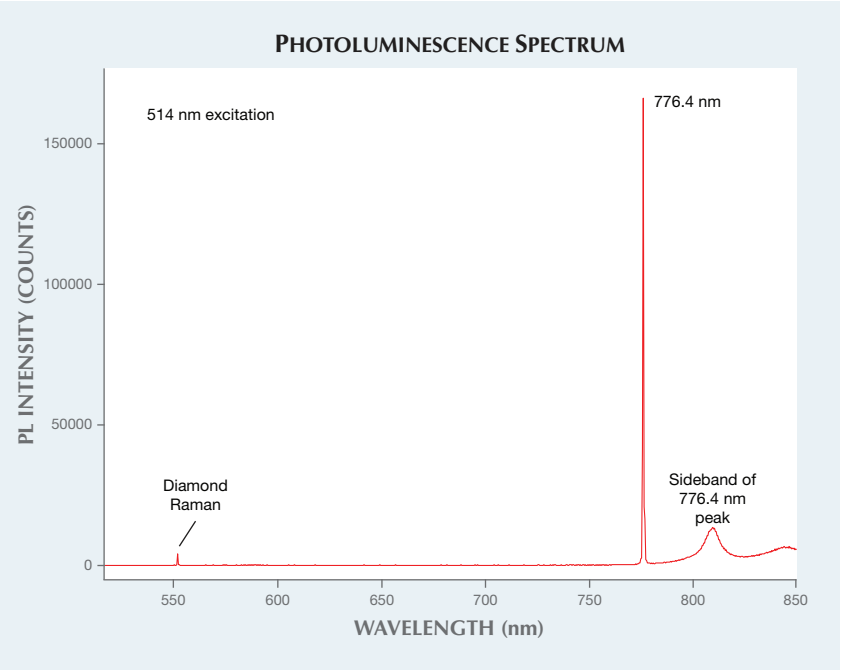

Figure 5. With 514 nm excitation and liquid-nitrogen temperatures, the 776 nm PL peak dwarfs the diamond Raman peak at 552.4 nm and all other PL features in the spectrum. The intensity ratio between the 776 nm peak and the diamond Raman peak is about 42:1.

using fluorescence spectroscopy. The 776.4 nm PL peak is observed when the diamond is at liquid-nitrogen temperatures, but it is outside the visible range and not excited at room temperature. Therefore, this near-infrared emission, while strong, does not contribute to the color of the diamond. The diamond's red phosphorescence, while subtle, may have been sufficient to introduce enough reddish component to render a purple color call (as opposed to the more common blue to violet). The singular occurrence of the very strong 776.4 nm PL peak and an unusual bodycolor for a type IIb diamond make this stone notable.

Sally Eaton-Magaña

FLUORITE Sphere with Phosphorescent Coating

A large green 2,685 ct sphere measuring 120 mm (figure 6, left) was recently examined in the Carlsbad lab.

Figure 6. This large fluorite sphere proved to be coated with a fine-grained phosphorescent powder and a colorless plastic.

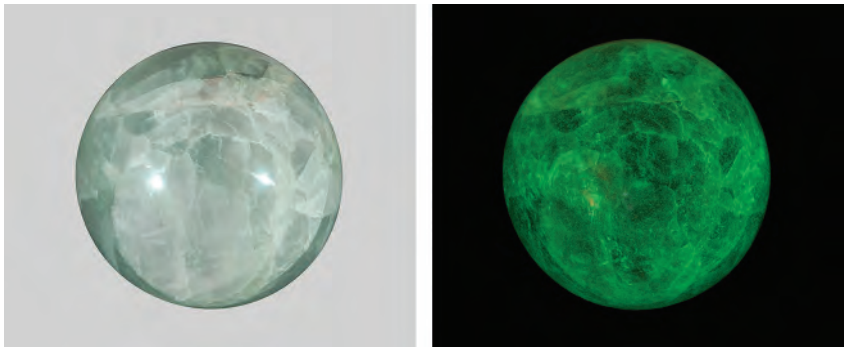

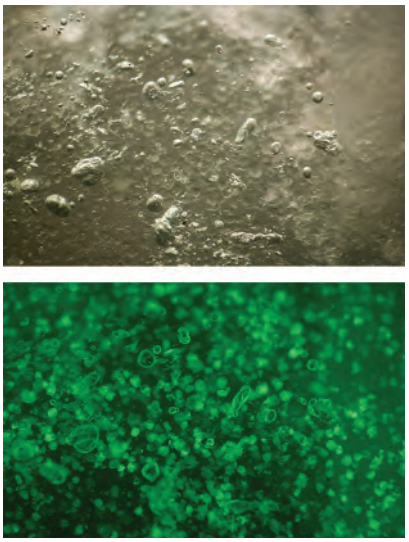

Figure 7. Gas bubbles were trapped in the colorless plastic coating of this "night glowing pearl" (top), and a granular material underneath the colorless coating was the source of the phosphorescence (bottom). Field of view 3.55 mm.

The sphere displayed an unusual phosphorescent reaction when exposed to a strong illumination source (figure 6, right). These phosphorescent stones are commonly referred to by the misnomer "night glowing pearl."

The sphere was warm to the touch. Microscopic examination revealed a colorless plastic coating, readily identifiable by the numerous gas bubbles trapped within (figure 7, top). Upon further inspection, a subsurface granular material that contributed a very subtle green component to the sphere's overall bodycolor was observed (figure 7, bottom). The granular material was also responsible for the material's phosphorescence. It was apparent from these observations that the colorless coating was used to adhere the fine-grained powder to the surface of the sphere. The coating acted as an enhancement, contributing a near-vitreous luster to the finished sphere. The stone also contained numerous cleavage cracks oriented in numerous unrelated directions, and fractures along grain boundaries indicative of a crys-

talline aggregate material. Because the fine-grained powder was coated with polymer, we were unable to analyze it for identification; however, the appearance was consistent with that of a strontium aluminate material that has been previously reported to coat "night glowing pearls" (Spring 2005 Lab Notes, pp. 46–47).

Due to the plastic coating, a refractive index measurement of the substrate material was not possible. Raman spectroscopy positively identified the substrate material as fluorite, which was consistent with the microscopic appearance.

While "night glowing pearls" have been characterized, this example was unique because of its large size and the fact that the phosphorescent reaction was easily induced by visible light. It was also unusual that the phosphorescent material was nearly invisible to the naked eye, creating the appearance of a normal, uncoated fluorite sphere.

Nathan Renfro

PEARLS

Assembled and Bead-Cultured

A cream and white baroque pearl weighing 10.27 ct (figure 8) was recently submitted with seven other pearls to the Bangkok laboratory for a GIA Quality Assurance Report, which provides rapid identification for sorting purposes. The pearl appeared to have been assembled, as it possessed an odd translucent ring at one end, indicating where separate components had been joined together.

Prior to examination with real-time microradiography, it seemed likely that a shell bead nucleus was hidden from view, as the banded structure of a shell was observed in the translucent area when viewed with transmitted light from a fiber-optic light source. The transparent bonding agent used to join the two parts also contained black impurities (figure 9, left). Obvious gas bubbles were visible with a loupe or gemological microscope. Out of scientific interest, the pearl was also examined with X-ray fluorescence and DiamondView imaging. X-ray fluorescence showed a strong reaction in the damaged and repaired area, as would be expected because of its thinner nacre coverage. DiamondView imaging revealed the banding within the bead, the dark inclusions in the bonding agent, and the bonding agent itself (figure 9, right).

Figure 8. The 10.27 ct baroque cultured pearl exhibited a suspicious translucent ring at one end.

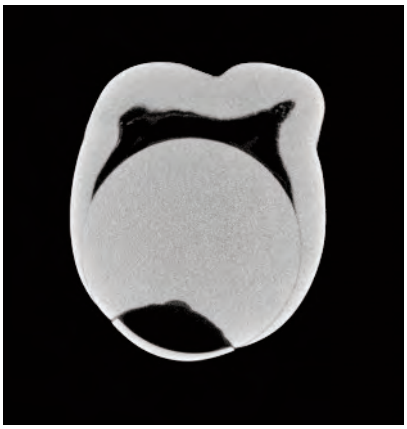

Figure 10. The broken bead and the nacreous cap applied to conceal the damage are clearly visible in this X-ray computed microtomography (μ-CT) slice.

Real-time microradiography revealed the bead nucleus as well as an extremely thin nacreous cap that had been used to cover the damaged bead. While X-ray computed microtomography (μ-CT) would not normally be needed to identify such an obviously bead-nucleated pearl, it was used to display the results with even greater clarity (figure 10). This analytical technique clearly showed the broken bead and an area where a new piece of nacre had been applied to repair the pearl. This would explain the mismatching translucent ring.

This study demonstrated how the internal secrets of pearls can be revealed by a variety of techniques.

Areeya Manustrong

Strong Pinkish Purple Freshwater Bead-Cultured Pearls

Freshwater cultured pearls are known for their wide range of attractive colors, including different combinations of white, orange, pink, and purple hues (S. Akamatsu et al., "The cur-

Figure 9. Left: Weak banding was faintly visible beneath the repaired and assembled area when viewed with a strong light source. Field of view 8 mm. Right: The banding was more noticeable in the DiamondView.

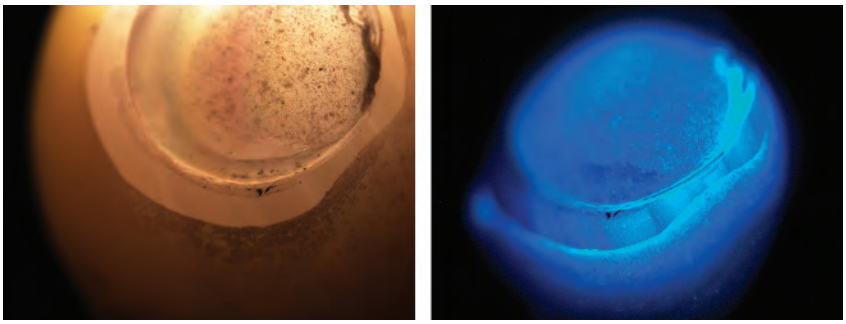

Figure 11. This necklace of freshwater bead-cultured pearls from China displays strong pinkish purple hues with orient.

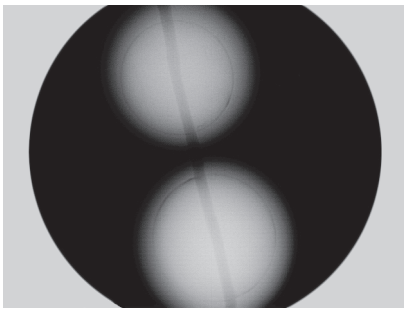

Figure 12. Real-time X-ray microradiography analysis revealed the round shell bead nucleus used to culture each of the pearls.

rent status of Chinese freshwater cultured pearls," Summer 2001 *G&G*, pp. 96–113). Jack Lynch of Sea Hunt Pearls (San Francisco) recently submitted a necklace consisting of 33 strong pinkish purple near-round pearls, ranging from 11.90 to 13.85 mm in diameter (figure 11), to GIA's New York laboratory. The unusually intense color and large size of the pearls immediately drew our attention. Mr. Lynch indicated that the pearls were farmed in both the Hunan and Hubei provinces of China, over a period of three and a half to four years.

Real-time X-ray microradiography (RTX) analysis revealed that all of the pearls in the necklace were bead cultured and had relatively thick nacre (figure 12). Energy-dispersive X-ray fluorescence (EDXRF) analysis detected a high concentration of manganese, confirming that these pearls were grown in a freshwater environment. Furthermore, Raman spectroscopy verified that their color was natural, with two strong peaks around 1130 and 1510 cm^{-1} associated with natural polyenic pigments found under 514 nm laser excitation (figure 13), consistent with previous studies (S. Karampelas et al., "Role of polyenes in the coloration of cultured freshwater pearls," *European Journal of Mineralogy*, Vol. 21, 2009, pp. 85–97).

Earlier Chinese production with large beads resulted in a high mortality rate. We continue to see larger bead-nucleated freshwater cultured pearls, so it appears that the process has greatly improved, either through better techniques or hybrid mollusks (D. Fiske et al., "Continuity and change in Chinese freshwater pearl culture." Summer 2007 *G&G*, pp. 138–145). Pearls with larger size, a near-round shape, and intense coloration are highly sought after and more valuable than traditional prod-

Figure 13. Raman spectroscopic analysis on the pearl's surface showed two natural polyenic pigment peaks at 1130 and 1510 cm^{-1}.

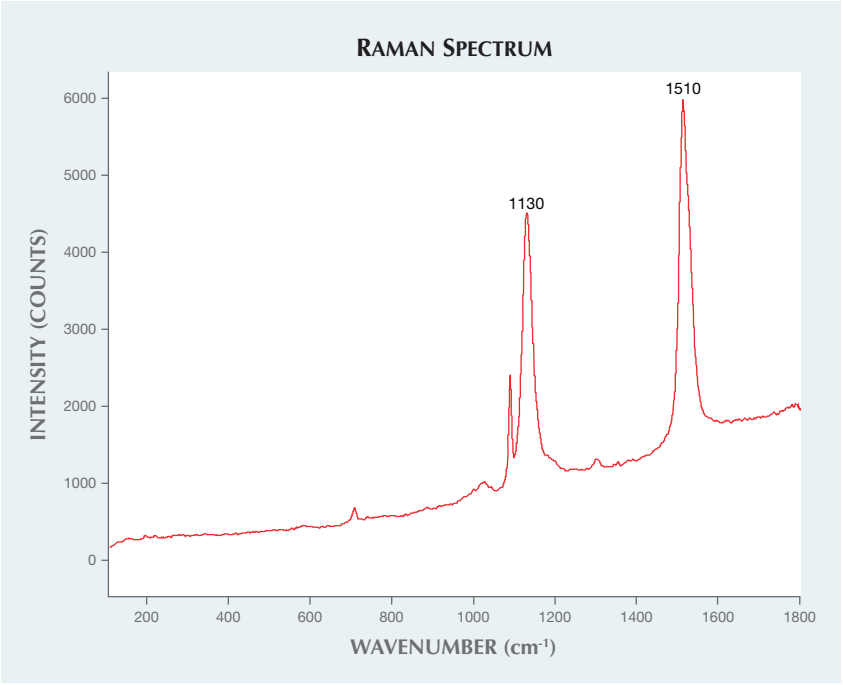

ucts. The owner's inquiries revealed that the pearls were formed under an extremely controlled environment and culturing procedures in mussels that produce the material marketed as "Edison pearls." This necklace proves that current culturing techniques can achieve a wide range of vibrant hues, providing interesting and unique products for the market.

Yixin (Jessie) Zhou and Chunhui Zhou

Beryllium-Diffused and Lead Glass–Filled Orange SAPPHIRE

The Carlsbad laboratory recently received a 4.25 ct transparent orange oval mixed-cut stone (figure 14) for a colored stone identification report. Standard gemological testing established the following properties: RI—1.762 to 1.770; birefringence—0.008; optic sign—uniaxial negative; pleochroism—strong orange and very light yellow; and SG—3.98. All of these properties are consistent with both natural and synthetic sapphire.

Under magnification, the most distinctive internal characteristic was the presence of numerous fractures partially healed by glassy flux-like droplets. Some had a wispy veil and fingerprint-like appearance. One fracture with large healed areas showed a strong flash effect, which appeared greenish blue under brightfield illumination (figure 15, left) and orange-red under darkfield illumination (figure 15, center) when rotating the stone to another direction. Under diffused lighting, the outline of the large partially healed areas stood out clearly (figure 15, right). The flash effect indicates that the fracture was healed using a material with a high refractive index, possibly lead glass (S. F. McClure et al., "Identification and durability of lead glass–filled rubies," Spring 2006 *G&G*, pp. 22–34).

Figure 14. This 4.25 ct orange sapphire was submitted for a colored stone identification report.

Heat-treated sapphires submitted to GIA are routinely checked using advanced analytical tools. Energy-dispersive X-ray fluorescence (EDXRF) analysis was performed on the table facet where the large healed fracture with flash effect was located. The presence of Pb was clearly detected, indicating the filler was lead glass. Laser ablation–inductively coupled plasma–mass spectrometry (LA-ICP-MS) was used to confirm the stone's natural trace-element chemistry and detect the beryllium-diffusion treatment. Beryllium was present in all laser ablation spots, but analysis of the partially healed fractures revealed high Pb content in addition to Be. In one spot, both high Be (156 ppmw) and Pb (23,300 ppmw) were present, which provided some possible insight into the treatment process.

Corundum selected for lead-glass filling usually goes through a two-step process. The material is heated at temperatures from 900° to 1400°C to remove the impurities in fissures, followed by another heating at 900° to 1000°C in the presence of a lead-glass mixture to fill the fractures (V. Pardieu, "Lead glass filled/repaired rubies," Asian Institute of Gemological Sciences Gem Testing Laboratory, 2005, http://fieldgemology.org/Ruby_lead_glass_treatment). Beryllium diffusion requires a temperature range from 1800° to 1850°C, close to corundum's melting temperature of 2045°C, which requires a special resistance furnace (J. L. Emmett et al., "Beryllium diffusion of ruby and sapphire," Summer 2003 *G&G*, pp. 84–135). If the stone had been filled first, the lead-glass filler likely would have melted and flowed out of the fractures during the beryllium diffusion treatment (McClure et al., 2006). It is unlikely that the Be diffusion and lead

Figure 15. Under brightfield illumination, the large healed fracture showed a greenish blue flash effect (left). Under darkfield illumination, the same fracture showed an orange-red flash effect (center). Under diffused lighting (right), the outline of the fracture became distinct. Field of view 3.45 mm.

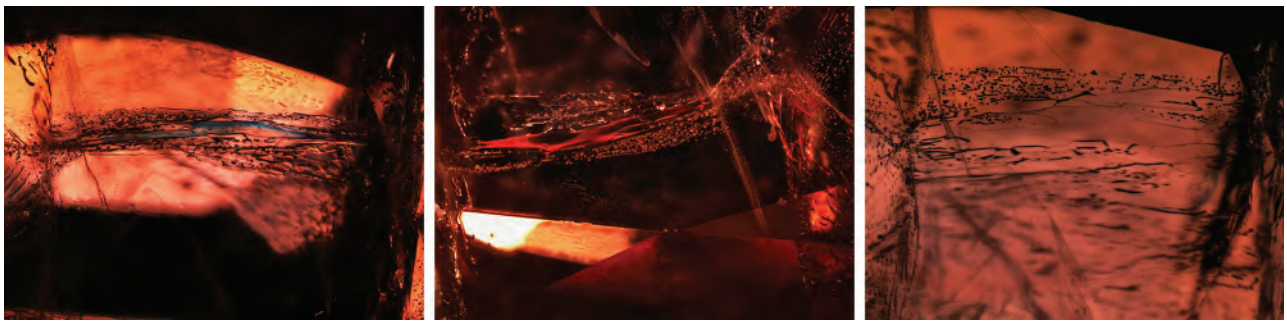

glass–filling treatments occurred simultaneously. Such a process has not been documented and would likely pose technical challenges, partly because the relatively high temperature required for the beryllium diffusion treatment would have outgassed much of the lead and caused serious toxic gas exposure.

The best possible explanation is that the stone was beryllium diffused at a high temperature to improve its color before being treated with lead glass at a lower temperature to improve its clarity. If some residue of the original Be treatment was left in a fracture that was later filled with lead glass, this could explain the correlation of high Be and high Pb in one of our LA-ICP-MS analyses.

GIA's laboratories have identified numerous beryllium-diffused or lead glass–filled stones. That the two treatments were applied in a single sapphire is very rare. It is the first time such a stone has been examined by the GIA laboratory.

Ziyin Sun

LPHT-Annealed Pink CVD SYNTHETIC DIAMONDS

Due to nitrogen vacancy and hydrogen complexes, as-grown CVD synthetic diamonds are usually brown, which are less desirable than other colors. Post-growth treatments such as high-pressure, high-temperature (HPHT) treatment and/or irradiation and annealing, are applied to these synthetics to create attractive colors. In the past, we have reported HPHT-treated and multi-step treated pink CVD synthetics. Recently, the New York lab examined three pink CVD-grown diamonds that were treated with the technique known as low-pressure, high-temperature (LPHT) annealing.

The 0.37 ct rectangle, 0.31 ct rectangle, and 0.25 ct round brilliant were graded as Fancy Deep brownish orangy pink, Fancy Deep brown-pink, and Fancy brown-pink, respectively (figure 16). They were classified as type Ib diamond containing single substitutional nitrogen atoms (N_s^0) with absorption bands at 1130 and 1344 cm^{-1} (figure 17). The 0.37 ct sample contained a VS_2-grade feather and a few burn marks on the main facets; otherwise, all three were very "clean." The DiamondView images showed typical orange fluorescence and linear growth striations, which are caused by uneven uptake of defects along the growth steps (again, see figure 16). The orange fluorescence is usually observed in N-doped CVD synthetics.

The mid-IR spectra revealed post-growth LPHT annealing treatment. In figure 17, the absorption bands of C-H stretching at 2810, 2870, 2900, 2937, 2948, and 3031 cm^{-1} are created by LPHT annealing (see Y. Meng et al., "Enhanced optical properties of chemical vapor deposited single crystal diamond by low-pressure/high-temperature annealing," *PNAS*, Vol. 105, No. 46, 2008, pp. 17620–17625). They were modified and shifted from the peaks of unstable hydrogenated amorphous carbon complexes and NVH^- defects during the annealing process. The 3123 cm^{-1} (NVH^0) band,

Figure 16. Three LPHT-annealed CVD synthetic diamonds: Fancy Deep brownish orangy pink 0.37 ct (top left), Fancy Deep brown-pink 0.31 ct (top middle), and Fancy brown-pink 0.25 ct (top right). Their DiamondView images (bottom row) show orange fluorescence with linear growth striations.

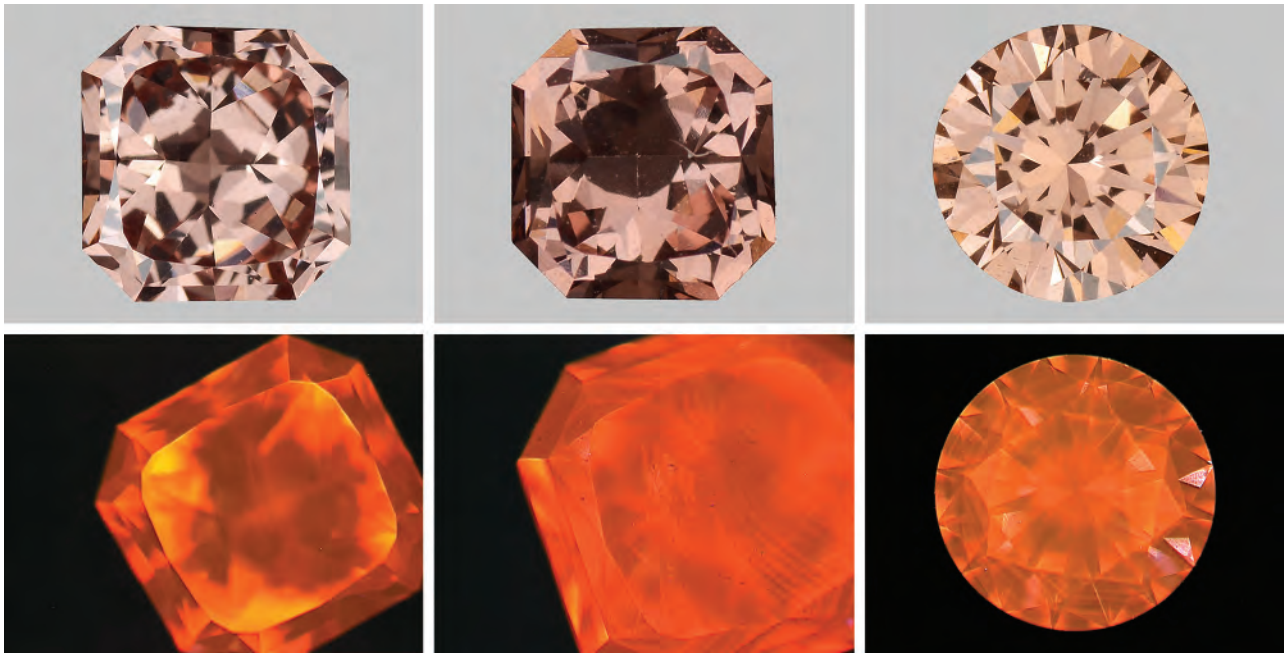

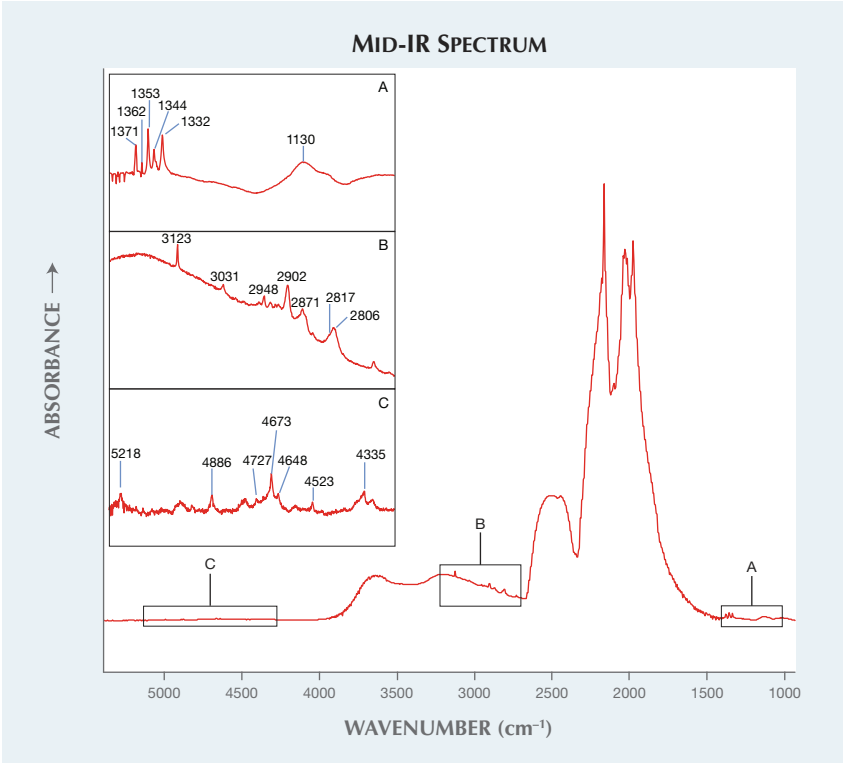

Figure 17. These CVD synthetics are classified as type Ib with N_s^0 atoms at 1130 and 1344 cm^{-1} (inset A). The LPHT annealing was revealed by C-H stretching bands, as seen in inset B. Additional unknown bands were also observed (inset C).

which is a common defect in as-grown CVD synthetic diamonds and annealed out by HPHT treatment, is present. This defect was detected in LPHT-annealed CVD synthetics (again, see Meng et al., 2008). The 3107 cm^{-1} (N3VH), which can be created by HPHT annealing in CVD synthetic diamonds, is absent. Positively charged single substitutional nitrogen atoms (Ns^+) were detected at 1332 cm^{-1}. Additionally, unknown bands were also detected at 1353, 1362, 1371, 4335, 4523, 4648, 4673, 4727, 4886, and 5218 cm^{-1}. A broad absorption band with absorption maxima at approximately 525 nm and sharp nitrogen-vacancy (N-V) centers at 575 nm (NV^0) and 637 nm (NV^-) in the visible-NIR spectrum are responsible for pink and orange color components in these samples (figure 18). The vivid orange fluorescence in DiamondView images are also attributed to N-V centers. The H3 center is observed at 503 nm. There are also unknown additional absorption bands at 419.5, 485.8, 495.1, 666.5, 685.4, 711.7, 753.1, 781.4, and 850.3 nm. Very strong N-V centers can be observed in the 514 nm PL spectra.

HPHT annealing can be achieved at temperatures ranging from 1800°–2500°C and pressures greater than 5 GPa. High pressure is required in order to prevent graphitization, especially in natural diamond. In contrast, LPHT annealing is performed at temperatures 1400–2200°C and pressures below 300 torr (<3.99 × 10^{-5} GPa, below atmospheric pressure) (again see Meng et al., 2008). Graphitization became significant above 2200°C. At temperatures above 700°C, vacancies started to move and were trapped at single substitutional nitrogen atoms, creating N-V centers; however, nitrogen atoms become mobile at temperatures above 1700°C, causing the N-V centers to anneal out. Therefore, strong N-V centers (which are much greater than the diamond Raman peak) in the 514 nm PL spectra of these samples suggested that they were annealed at temperatures below 1700°C. Lack of a peak at 3107 cm^{-1} is also suggestive of an annealing temperature below 1700°C. This upper temperature limit is further supported by presence of a band at 3123 cm^{-1}, which can be annealed out at above 1800°C. Incorporation of H3 center occurs above 1500°C; thus, annealing temperatures for these samples can be proposed as 1500°C < T < 1700°C. According to Meng's experiment, this temperature range can be correlated with pressure from 150 to 200 torr, with annealing time from 10 to 720 minutes.

Brown as-grown CVD synthetics have been changed to brownish pink by LPHT annealing for 15 minutes by Meng et al. (2008); they were also able to improve colorless CVD-grown diamonds by an average of three color grades. LPHT treatment may have created the attractive pink hue in these samples, although it could not completely eliminate the brown coloration. We expect to encounter more LPHT-treated diamonds in the future.

Kyaw Soe Moe, Ulrika D'Haenens-Johansson, and Wuyi Wang

Near-Colorless Melee-Sized HPHT Synthetic Diamonds Identified in GIA Laboratory

With significant development in diamond treatments and synthesis over the last decade, the trade has serious concerns about treated and/or synthetic material mixed with natural melee-sized stones. The mixing of treated and synthetic diamonds with yellow natural melees was previously reported (Winter 2014 Lab Notes, pp. 293–294; Spring 2015 Lab Notes, pp. 64–65). In order to ensure consumer confidence, it is essential to screen melees so as to distinguish all treated and synthetic goods.

Recently, the Bangkok lab had the opportunity to examine six melee-sized specimens submitted for synthetics and treatment screening. The

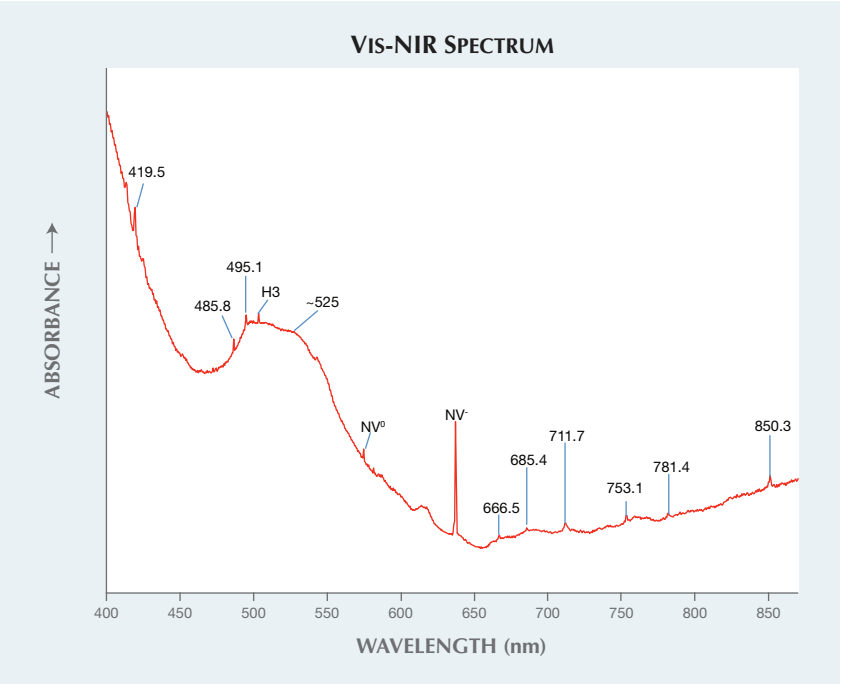

Figure 18. Absorption maxima at approximately 525 nm and N-V centers are responsible for the pink color in these samples. The H3 center can be observed, along with many unknown bands.

transparent, near-colorless round brilliants ranged in size from 0.005 to 0.01 ct (figure 19). Microscopic observation revealed no obvious inclusions. Between crossed polarizing filters, very little or no strain was observed. Infrared absorption spectra showed that four of the samples were type IIa diamonds with no detectable defect-related absorption, while the other two were type IIb diamonds accompanied by uncompensated boron showing moderately strong absorption at approximately 2800 cm^{-1}. Photoluminescence spectra obtained at liquid-nitrogen temperature with 514 and 633 nm laser excitations revealed an emission doublet of the negatively charged silicon split-vacancy defect $[Si\text{-}V]^-$ at 736.6/736.9 nm for five of the samples, while 830 nm laser excitation showed an emission doublet at 883.0/884.7 nm owing to a nickel-related defect for all six samples (figure 20). DiamondView imaging revealed either blue or green fluorescence, together with characteristic growth features of HPHT synthesis, as seen in figure 21. Strong blue phosphorescence was also observed for all six samples. These gemological and spectroscopic features confirmed that the specimens were grown by HPHT synthesis.

To the best of our knowledge, this is the first examination of near-colorless HPHT synthetics of these sizes by a gemological laboratory. Discovery of these HPHT synthetic diamond melee reaffirms the need to screen the huge volume of near-colorless melee currently in the trade.

Wasura Soonthorntantikul and Piradee Siritheerakul

Phosphorescence of SYNTHETIC SAPPHIRE

Phosphorescent features in synthetic colorless sapphires have previously been reported in *G&G* (Fall 2013 GNI, pp. 182–183). A 1.14 ct colorless sample was recently submitted to the New York lab for identification (figure 22, left). The gemological properties determined the stone was corundum. The specimen was free of inclusions, with no detectable gas bubbles or curved striae. Quantitative chemical analysis, showing a lack of gallium as well as iron levels below the detection limit, indicated that the sample was synthetic. The material was also transpar-

Figure 19. These six near-colorless round brilliant melee, ranging from 0.01 to 0.005 ct, proved to be HPHT synthetic diamonds.

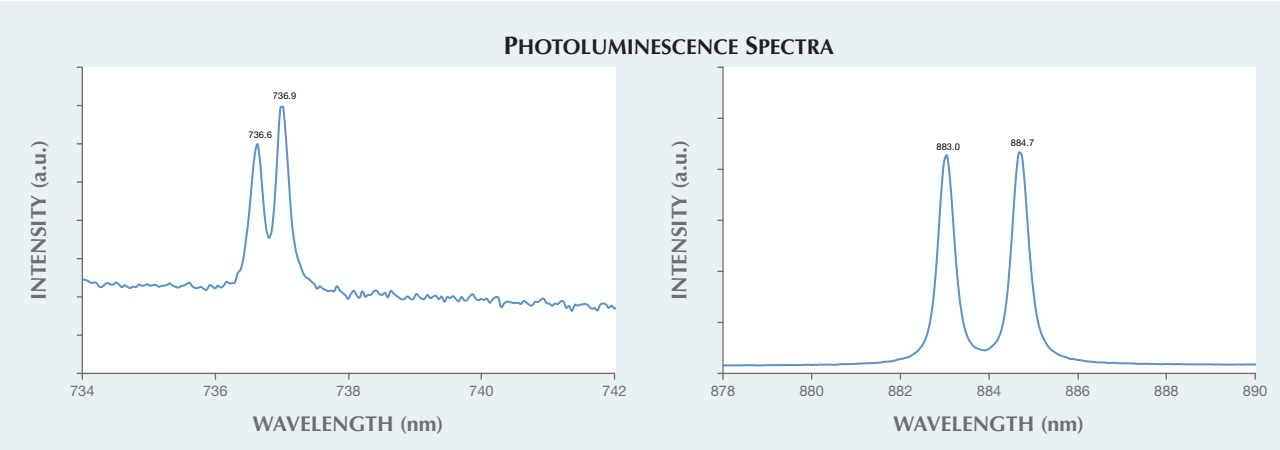

Figure 20. Photoluminescence spectra at liquid-nitrogen temperature of a small near-colorless HPHT synthetic diamond. The spectra displayed emission peaks at 736.6 and 736.9 nm related to a [Si-V]⁻ defect (left, 514 nm laser excitation) and at 883.0 and 884.7 nm associated with a Ni-related defect (right, 830 nm laser excitation).

ent to short-wave ultraviolet radiation, whereas natural colorless sapphires do not transmit short-wave UV light due to the quenching effect from trace impurities (S. Elen and E. Fritsch, "The separation of natural from synthetic colorless sapphire," Spring 1999 *G&G*, pp. 30–41). This is the same test used to effectively separate type I and II diamonds; nitrogen impurities in diamonds are strong absorbers of light in the short-wave UV range between 225–320 nm (C. M. Breeding, "The 'type' classification system of diamonds and its importance in gemology," Summer 2009 *G&G*, pp. 96–111). The UV-visible spectrum shown in figure 23 also illustrates the transparency with the absorption edge at approximately 216 nm, whereas natural near-colorless sapphires typically have an absorption edge around 300 nm.

Figure 24 illustrates the phosphorescence band centered at approximately 424 nm, along with other minor decay bands observed in the visible spectrum that mix together to produce the blue phosphorescence observed in figure 22 (right). The phosphorescence lasted about 25 seconds, until the excited electrons dissipated. The only trace elements detected with LA-ICP-MS were Ti (21 ppma average), and Cr, Mg, and Ca (below 5 ppma). Chalky blue fluorescence in sapphires is believed to be due to Ti^{4+} charge-transfer transition of isolated Ti^{4+} ions or Ti-Al vacancy pairs. The fluorescence peak is usually between 410 and 420 nm, but shifts to higher wavelengths as Ti concentrations increase (B. D. Evans, "Ubiquitous blue luminescence from undoped synthetic sapphire," *Journal of Lumines-*

Figure 21. This DiamondView image of one sample (third from the left in figure 19) shows the characteristic growth features of HPHT-grown synthetic diamonds.

Figure 22. Left: The 1.14 ct synthetic sapphire under daylight-equivalent lighting. Right: The sample exhibited phosphorescence in this DiamondView image.

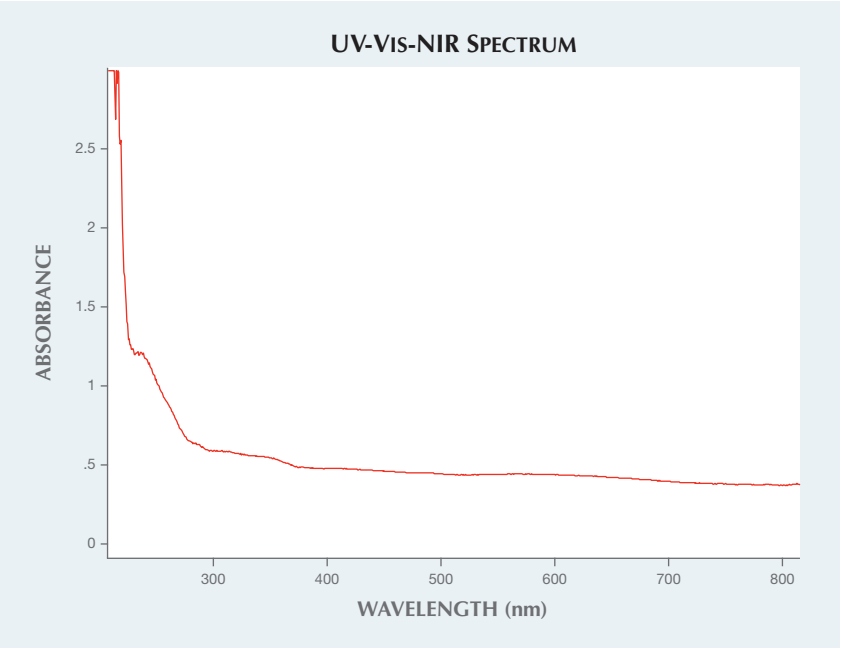

Figure 23. Transparency was observed in the UV-Vis-NIR spectrum.

cence, Vol. 60–61, 1994, pp. 620–626; W.C. Wong et al., "Charge-exchange processes in titanium-doped sapphire crystals. I. Charge-exchange energies and titanium-bound exitons," *Physical Review B*, Vol. 61, No. 9, 1995, pp. 5682–5698). The phosphorescence in synthetic colorless sapphires could be related to this property, with the addition of the decay route including forbidden energy transition states. Phosphorescence in synthetic colorless sapphires is still not well understood, and additional research is needed to verify the origin of this phenomenon.

Figure 24. The phosphorescence spectrum of the synthetic sapphire shows the main band centered at approximately 426 nm, along with smaller bands in the visible-light region.

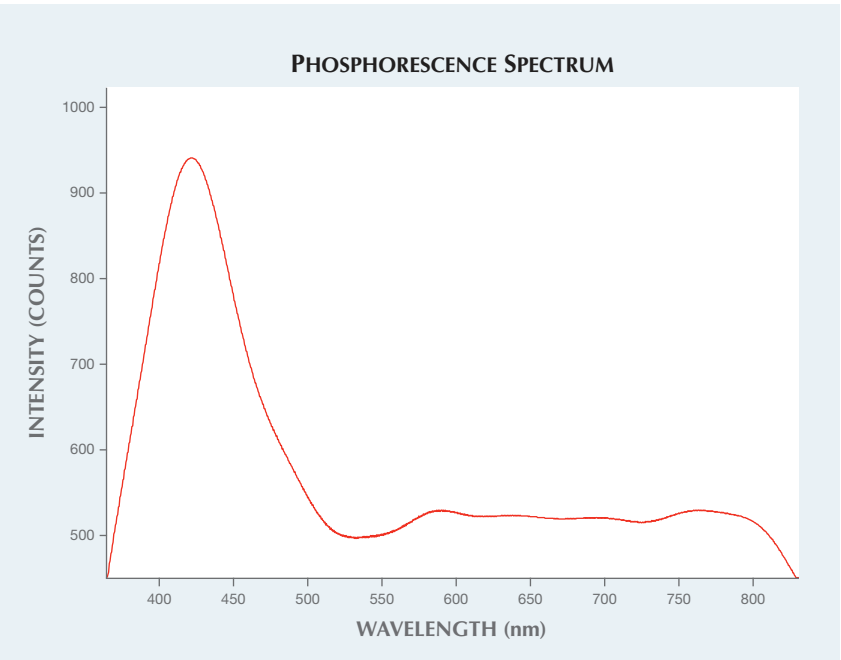

Akhil Sehgal

Chemical Analysis of ZIRCON

Radioactive elements such as thorium and uranium existed at higher concentrations during earlier ages of the earth; crystal formations from these periods were therefore more susceptible to acquiring higher concentrations of these materials. Zircon has a particular affinity for attracting rare earth elements such as uranium and thorium into its crystal structure due to similarities in the three elements' cation sizes, which allows U and Th to substitute for Zr in the crystal lattice, and other bonding properties such as coordination, electronegativity, and cation change. The isotopes break down through radioactive decay, releasing harmful doses of radiation to the host crystal. This destroys the crystal structure of zircon until it is nearly amorphous, in a process called metamictization (J.A. Woodhead, "The metamictization of zircon: Radiation dose-dependent structural characteristics," *American Mineralogist*, Vol. 76, 1991, pp. 74–82).

In gemology, zircon is categorized by the degree of radioactive degradation that has taken place. Highly degraded material with little to no crystal structure remaining is termed "low" or "metamict" zircon. "High" zircon is crystalline and nearly unaffected by radiation, while "intermediate" zircon is semi-crystalline, between the amorphicity of low zircon and the ordered crystalline structure of high zircon.

Five zircon samples were analyzed in this study based on their apparent crystallinity (figure 25). Raman spectroscopy shows the degradation of the crystal structure from its original structure, which can be illustrated by comparing it to zircon that has not been affected by radiation (figure 26). Infrared spectra (figure 27) also show

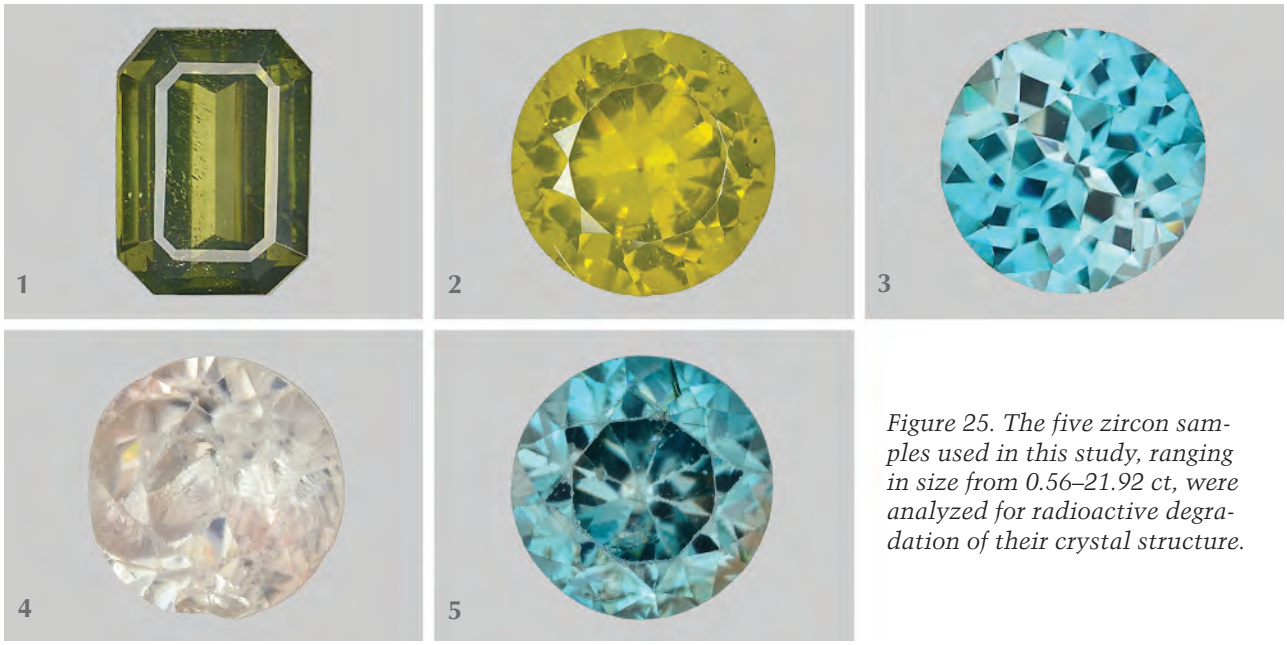

Figure 25. The five zircon samples used in this study, ranging in size from 0.56–21.92 ct, were analyzed for radioactive degradation of their crystal structure.

differences between the low and high zircons, as the former displays peak broadening and baseline irregularities.

Trace-element analysis of high and low/intermediate zircon using LA-ICP-MS illustrated variations in concentrations of several elements, including thorium, uranium, and lead. While uranium and thorium are easily incorporated into the crystal structure, the same is not true for lead, which can only appear in zircon as the byproduct of the radioactive decay chains of thorium and uranium. Due to this property, scientists have been able to accurately date zircons and Earth's age using isotope ratio analysis by comparing the lead to uranium ($^{238}U/^{206}Pb$) and lead to thorium ($^{232}Th/^{208}Pb$) ratios. These results showed the low zircon samples to be far older than the high zircon. Isotopic elemental analysis using LA-ICP-MS (table 1) determined that the low zircon was approximately a billion years old. This is far older than the high zircon samples, which were determined to be approximately 100 million years old. The higher content of radioactive elements earlier in Earth's formation, along with the longer period of time for metamictization to occur, contributed to the structures of the low zircons.

Figure 26. Raman analysis of samples 2 and 4, illustrating the difference between "low" and "high" zircons. Low zircon displaying amorphicity by peak loss and broadening.

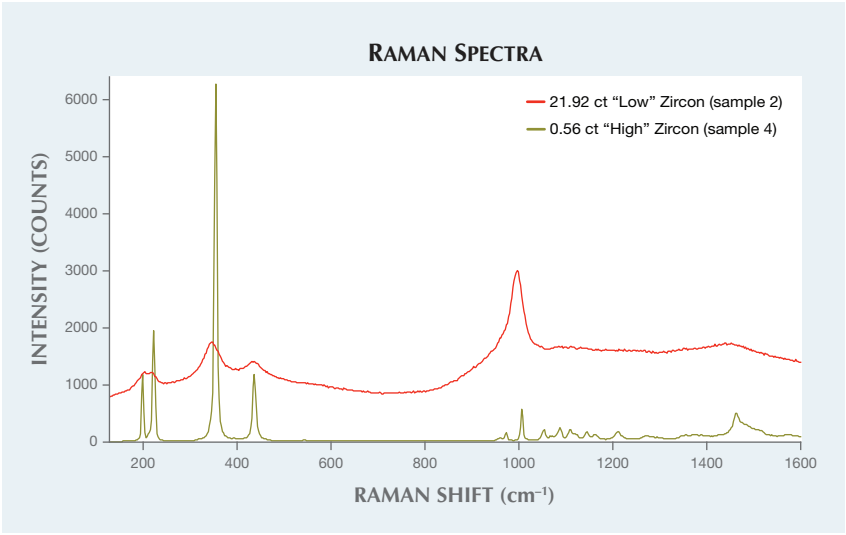

Trace-element analysis combined with spectroscopy can also detect treatments in zircon. Heat treatment, which is commonly performed on all types of zircon for color modification, can reestablish the crystal structure that was originally destroyed by natural processes. Zircon crystals with high lead content must have experienced a considerable amount of radiation exposure, leading to their lower crystalline order. High-lead zircon samples that show an ordered crystalline structure could have initially been low or intermediate and heat treated to restore the crystal structure. By correlating the trace-element chemistry with other analytical tools such as Raman spectroscopy, it may be possible to determine heat treatment of some types of zircons.

TABLE 1. Isotopic elemental analysis of zircon using LA-ICP-MS.

Sample	Weight	^{206}Pb	^{208}Pb	^{232}Th	^{238}U
(1) Greenish yellow "low" zircon	16.32 ct	848.40	54.53	237.10	4529.00
(2) Greenish yellow "low" zircon	21.92 ct	636.67	24.67	603.00	2083.33
(3) Greenish blue "high" zircon	10.14 ct	bdl*	bdl*	51.83	73.17
(4) Near-colorless "high" zircon	0.56 ct	0.81	0.63	200.00	210.17
(5) Blue "high" zircon	1.96 ct	0.12	0.19	85.02	99.98

** Below detection limit.*

Nearly all blue and near-colorless zircons have undergone heat treatment, as these colors are rarely found in nature; the majority of zircon rough is brown. The blue color of zircon is theorized to come from the chromophore U^{4+} cations, depending on how the uranium cations interact within the crystal structure. "Electric" blue zircon's color is typically produced by heating the stone to 1000°C in a reducing environment, while near-colorless material is produced at about the same temperature in an oxidizing environment. Heat treatment of zircons that have not had significant radiation damage can restore the crystallinity at the temperatures used for color modification treatments. Although very metamict zircons must undergo higher temperatures and longer duration of heating to restore a degree of crystallinity, these zircons will never achieve the electric blue color. It is difficult to even produce gem-quality material from this material. Zircon with poor crystallinity has more variation in polycrystalline grain orientation, bond length, element location, and bonding, as well as varying amorphicity. Knowledge of zircon's chemistry can facilitate the identification of treatments and growth conditions, and can be applied to determine various correlations pertaining to color and origin.

Akhil Sehgal

Figure 27. FTIR spectra of the zircon samples. The metamict zircons, samples 1 and 2, display an undefined baseline and broader bands than the high zircons.

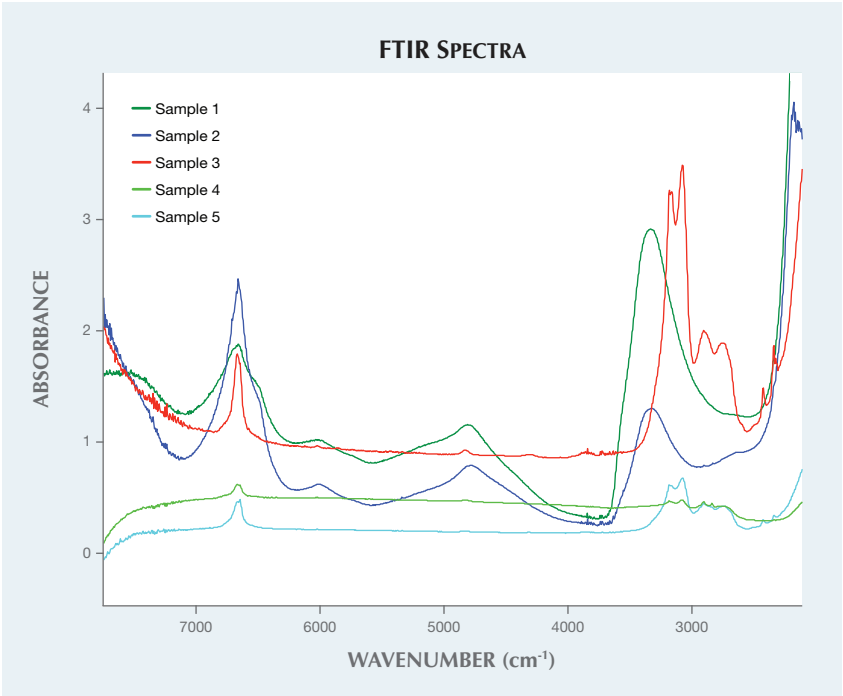

PHOTO CREDITS:
Jian Xin (Jae) Liao—1, 11, 16 (top right), 25; Paul Johnson—2; Robison McMurtry—4, 14; Don Mengason—6; Nathan Renfro—7; Nuttapol Kitdee—8, 19; Areeya Manustrong—9; Yixin (Jessie) Zhou—12; Ziyin Sun—15; Sood Oil (Judy) Chia—16 (top left and middle), 22 (left); Kyaw Soe Moe—16 (bottom); Charuwan Khowpong—21; Akhil Sehgal—22 (right).